Electronic Supplementary Material (ESI) for Journal of Materials Chemistry A.

Supplementary Information for

Hybrid palladium nanoparticles and nickel single atom catalyst for efficient electrocatalytic ethanol oxidation

Si Li,[a] Anxiang Guan,[a] Huining Wang,[a] Yaqin Yan,[a] Haoliang Huang,[b] Chao Jing,[b] Lijuan Zhang,[a] Linjuan Zhang,*[b] Gengfeng Zheng*[a]*

[a]Laboratory of Advanced Materials, Department of Chemistry and Shanghai Key Laboratory of Molecular Catalysis and Innovative Materials, Faculty of Chemistry and Materials Science, Fudan University, Shanghai 200438, China.

Email address: zhanglijuan@fudan.edu.cn, gfzheng@fudan.edu.cn

[b]Key Laboratory of Interfacial Physics and Technology, Shanghai Institute of Applied Physics Chinese Academy of Sciences, Shanghai 201800, China

Email address: zhanglinjuan@sinap.ac.cn

Methods

Chemicals. Nickel (II) chloride hexahydrate ($NiCl_2 \cdot 6H_2O$, Aldrich), copper (II) chloride dihydrate ($CuCl_2 \cdot 2H_2O$, Aldrich), sucrose ($C_{12}H_{22}O_{11}$, Aldrich), sulfuric acid (H_2SO_4, Sinopharm), sodium chloride (NaCl, Aldrich), palladium (II) chloride ($PdCl_2$, Aldrich), sodium borohydride ($NaBH_4$, Aldrich), ethanol (C_2H_5OH, Sinopharm), potassium hydroxide (KOH, Sinopharm).

Electrochemical measurements. The electrochemical measurements were conducted on an electrochemical workstation (CH Instruments, CHI 660) in a three-electrode system with 40 mL solution of 1 M KOH with 1 M ethanol as the electrolyte. A glassy carbon electrode (diameter of 3 mm) and a Pt wire were employed as the working and counter electrodes, respectively. 5 mg catalyst was dispersed in 1 mL acetone, with 60 μL of 5 wt% Nafion added subsequently. 10 μL of the solution was dripped on the surface of glassy carbon electrode. The Ag/AgCl (3 M KCl) electrode was used as the reference electrode. In addition, the electrochemical surface areas (ECSAs) and electrochemical impedance spectroscopy (EIS) tests were carried out in the above three-electrode system with 1 M KOH solution as the electrolyte. The liquid products of EOR were detected by ^{1}H NMR with dimethylsulfoxide (DMSO) dissolved in D_2O as the internal standard on Bruker AVANCEAV III HD 500. The Faradaic efficiency (FE) values of C_2 (acetate and acetaldehyde) and C_1 products were calculated as following:

$$FE_{C2} = \frac{n \times c \times V_{liquid} \times F}{Q_{liquid}} \times 100\%$$

$$FE_{C1} = 100\% - FE_{C2}$$

where *n* is the number of transferred electrons, *F* is the Faraday constant, V_{liquid} is the volume of electrolyte, and Q_{liquid} is the quantity of applied electric charges during the chronoamperometric measurements of EOR.

The ECSA values of the catalysts were calculated from the following formula:

$$ECSA(m^2 \cdot g^{-1}) = \frac{Q_{PdO}\,(mC)}{0.405\,(mC \cdot cm^{-2}) \times m_{Pd}(mg)} \times 0.1$$

The ECSA values of Pd NPs@Ni SAC, Pd NPs@Cu SAC, and Pd NPs@C were calculated as 84.7, 66.7 and 58.9 $m^2 \cdot g^{-1}$ respectively.

Supplementary Figures

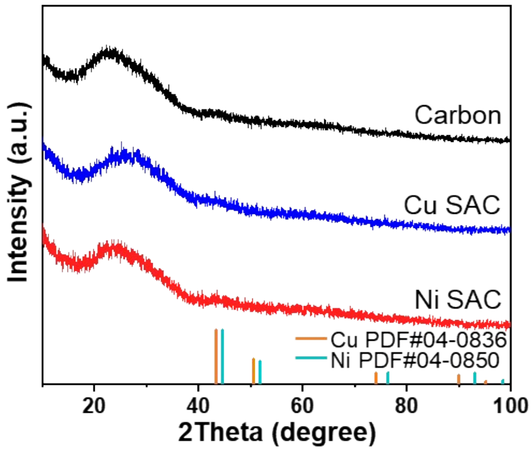

Figure S1. X-ray diffraction (XRD) patterns of Ni SAC, Cu SAC, and carbon substrate without metal elements.

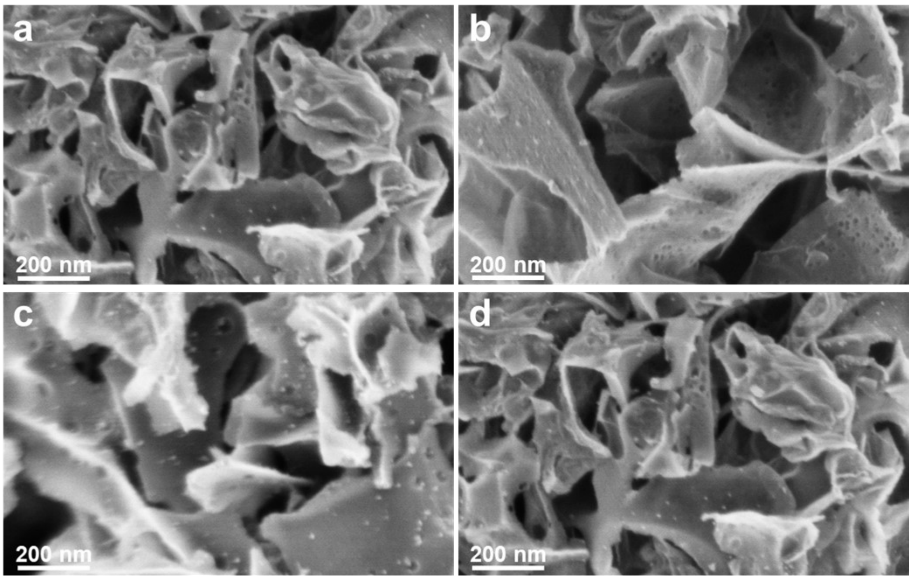

Figure S2. SEM images of (a) Pd NPs@Ni SAC, (b) Ni SAC, (c) Pd NPs@C, and (d) Pd NPs@Cu SAC.

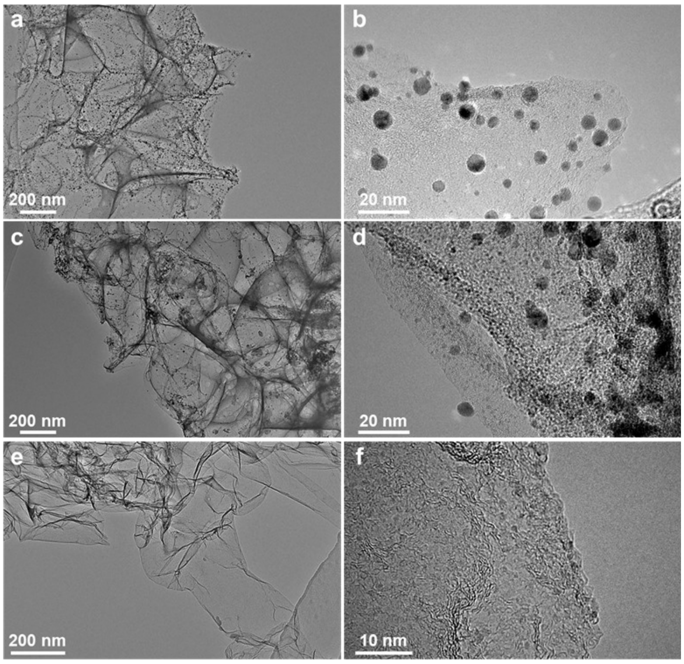

Figure S3. TEM images of (a, b) Pd NPs@C, (c, d) Pd NPs@Cu SAC, and (e, f) Ni SAC.

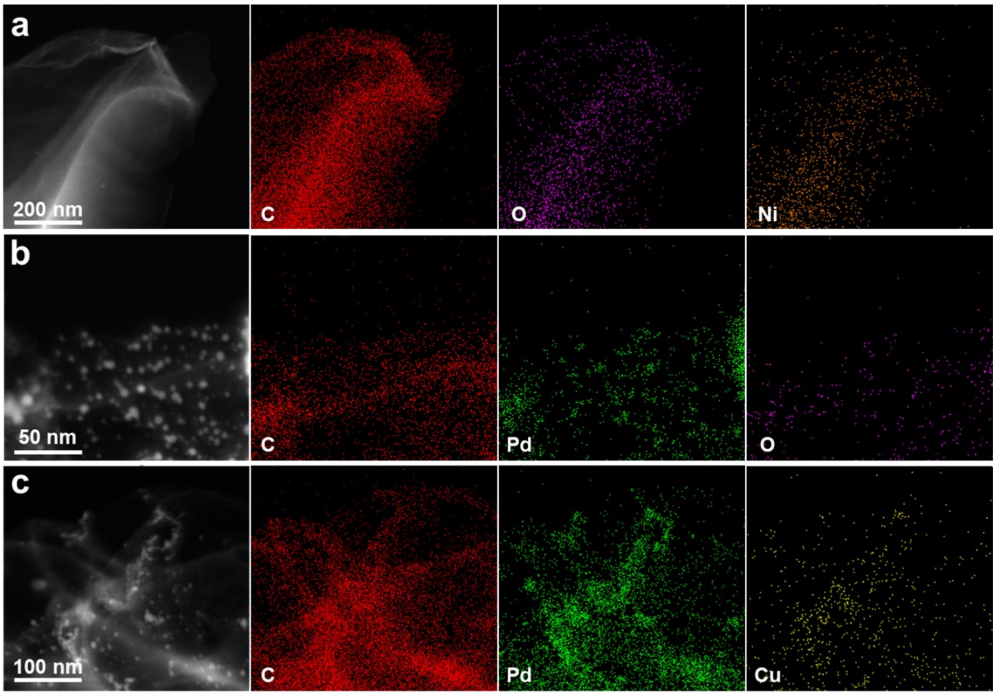

Figure S4. STEM images and corresponding elemental mappings of (a) Ni SAC, (b) Pd NPs@C, and (c) Pd NPs@Cu SAC.

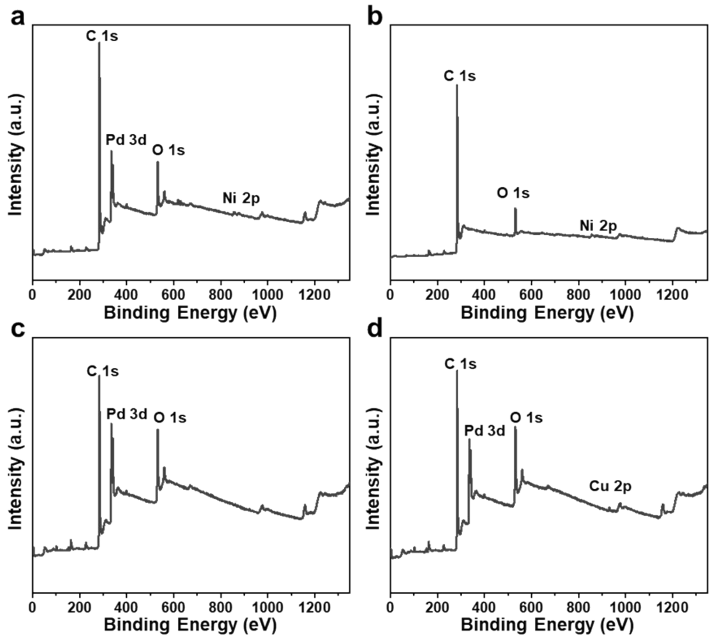

Figure S5. Overall survey scans of (a) Pd NPs@Ni SAC, (b) Ni SAC, (c) Pd NPs@C, and (d) Pd NPs@Cu SAC.

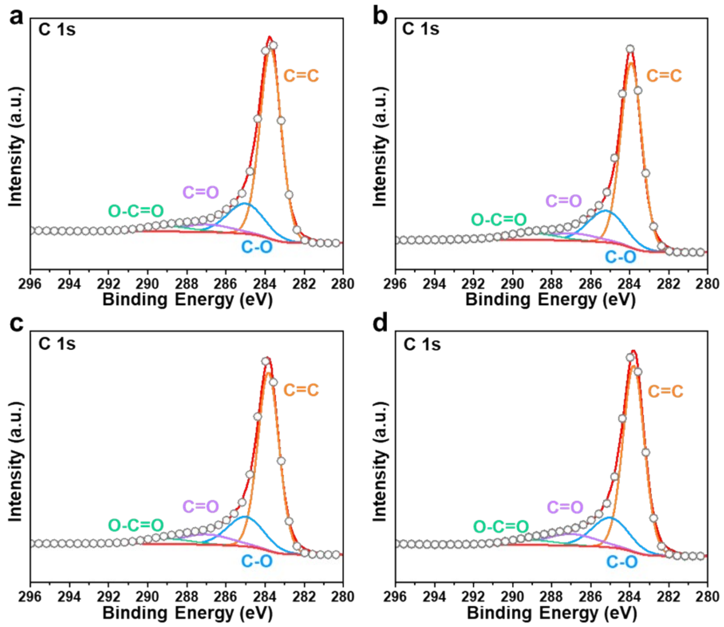

Figure S6. C 1s XPS spectra of (a) Pd NPs@Ni SAC, (b) Ni SAC, (c) Pd NPs@C, and (d) Pd NPs@Cu SAC.

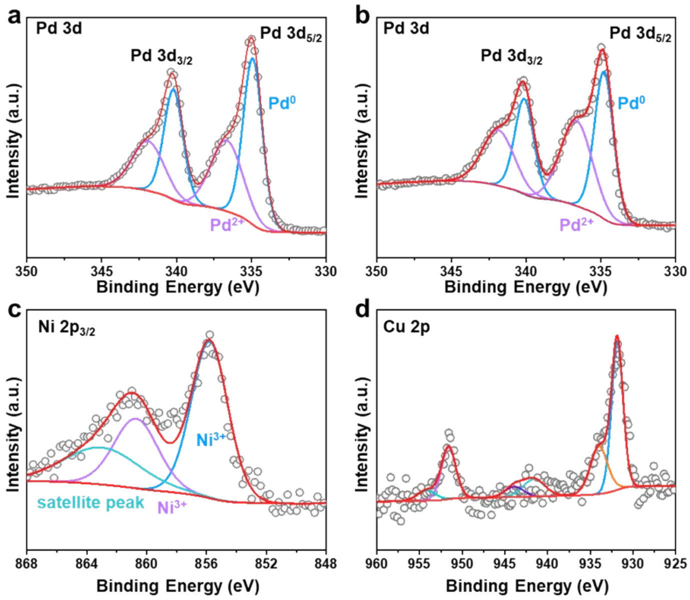

Figure S7. (a, b) Pd 3d XPS spectra of (a) Pd NPs@C and (b) Pd NPs@Cu SAC. (c) Ni 2p XPS spectra of Ni SAC. (d) Cu 2p XPS spectra of Pd NPs@Cu SAC.

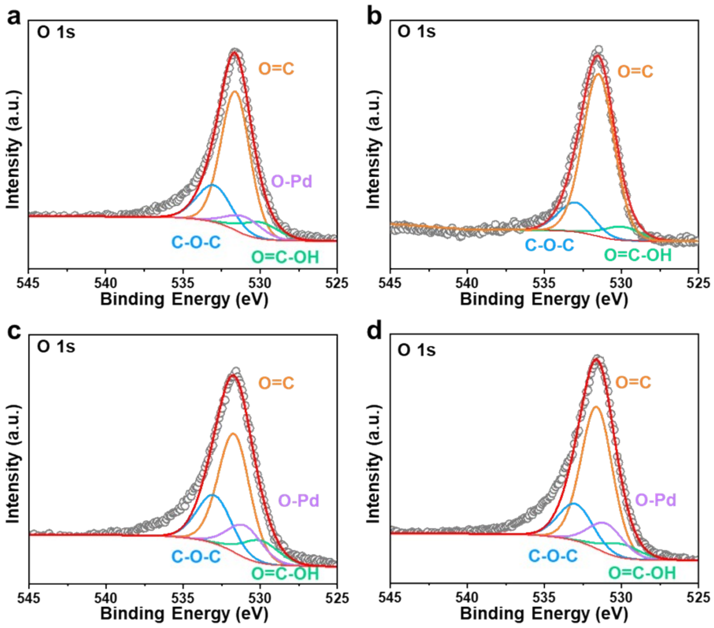

Figure S8. O 1s XPS spectra of (a) Pd NPs@Ni SAC, (b) Ni SAC, (c) Pd NPs@C, and (d) Pd NPs@Cu SAC.

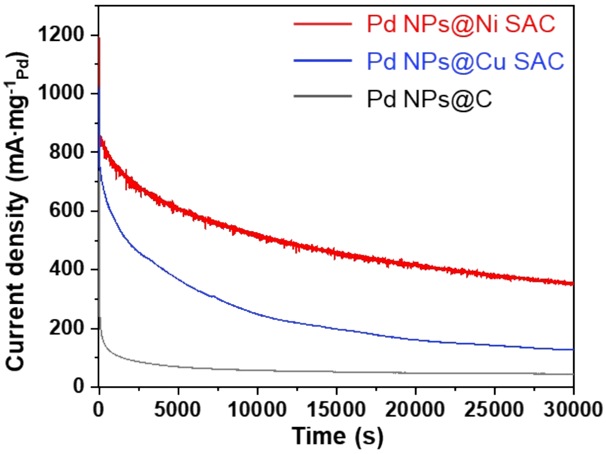

Figure S9. The chronoamperometric measurements of Pd NPs@Ni SAC, Pd NPs@Cu SAC and Pd NPs@C at 0.92 V (vs. RHE).

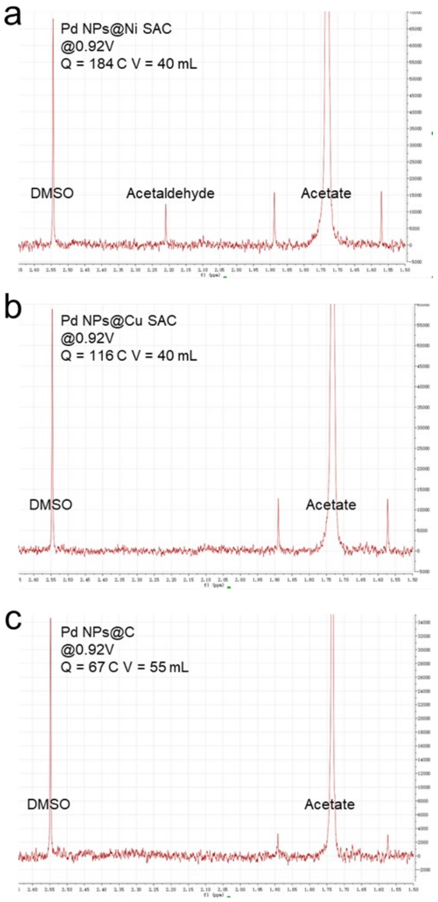

Figure S10. ^{1}H-NMR data of the electrochemical reaction products.

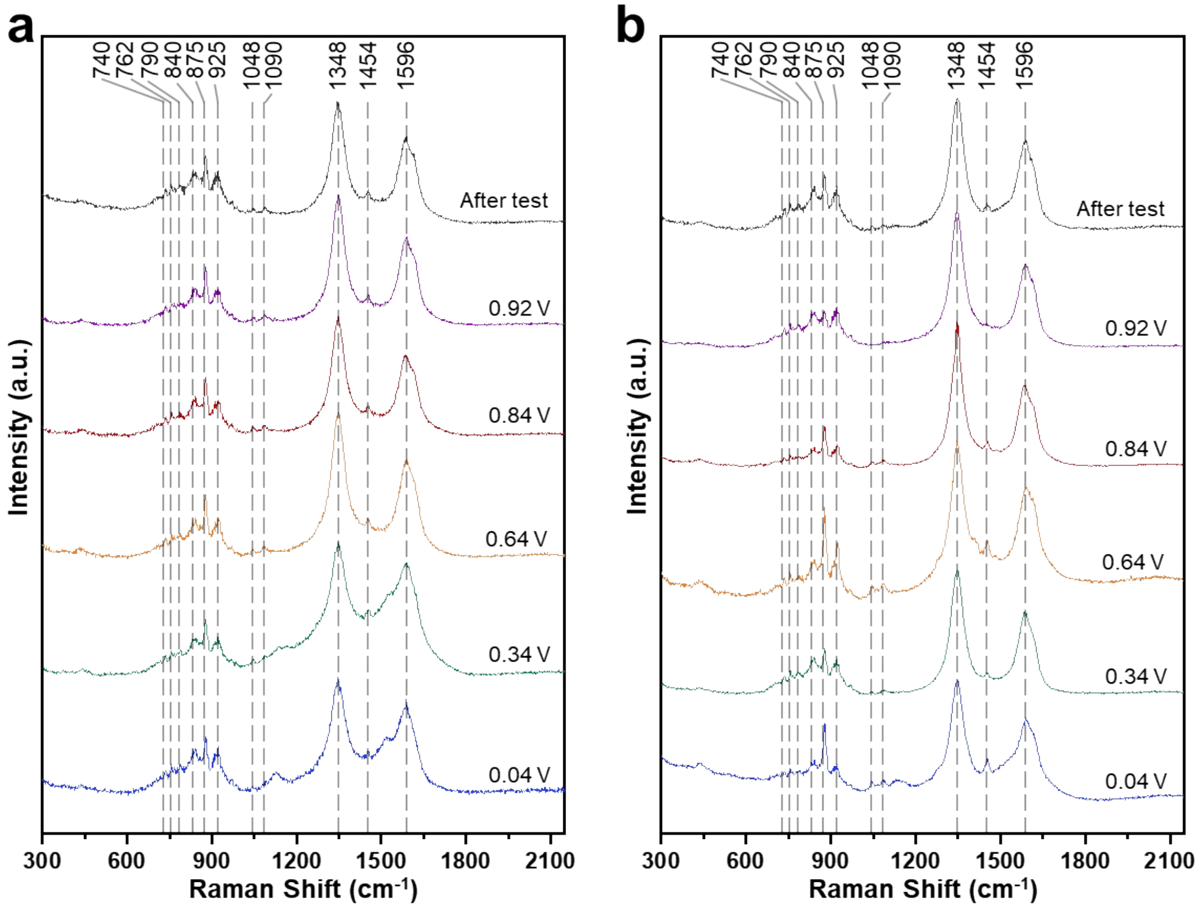

Figure S11. Operando electrochemical Raman spectra of chemical changes occurred during the ethanol oxidation on (a) Pd NPs@Cu SAC and (b) Pd NPs@C.

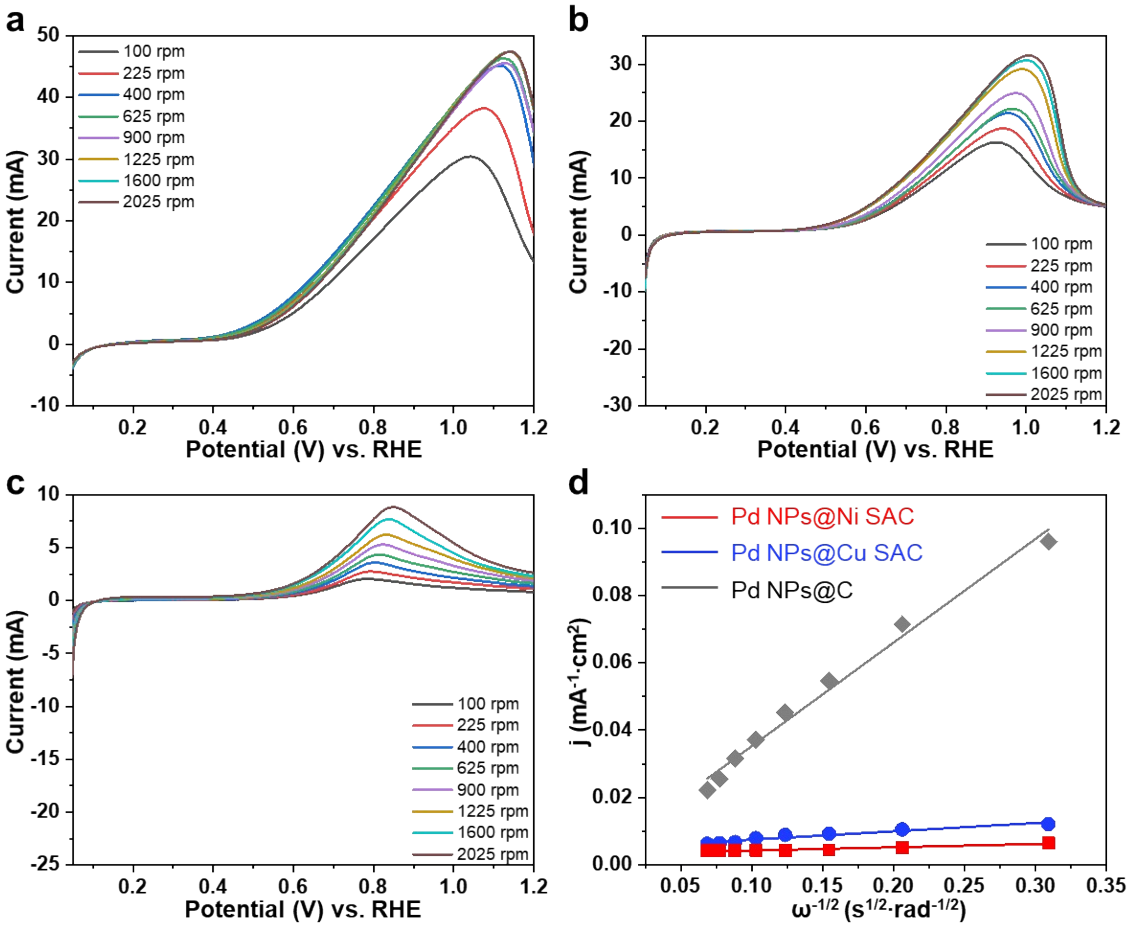

Figure S12. Polarization curves of (a) Pd NPs@Ni SAC, (b) Pd NPs@Cu SAC, and (c) Pd NPs@C with a rotating disk electrode at 100 mV·s^{-1} in 1 M KOH. (d) Absolute value of *j* against the square root of the rotation rate (i.e., the Levich plot). Straight lines were fitted to the data demonstrating well-defined mass transport under the test conditions.

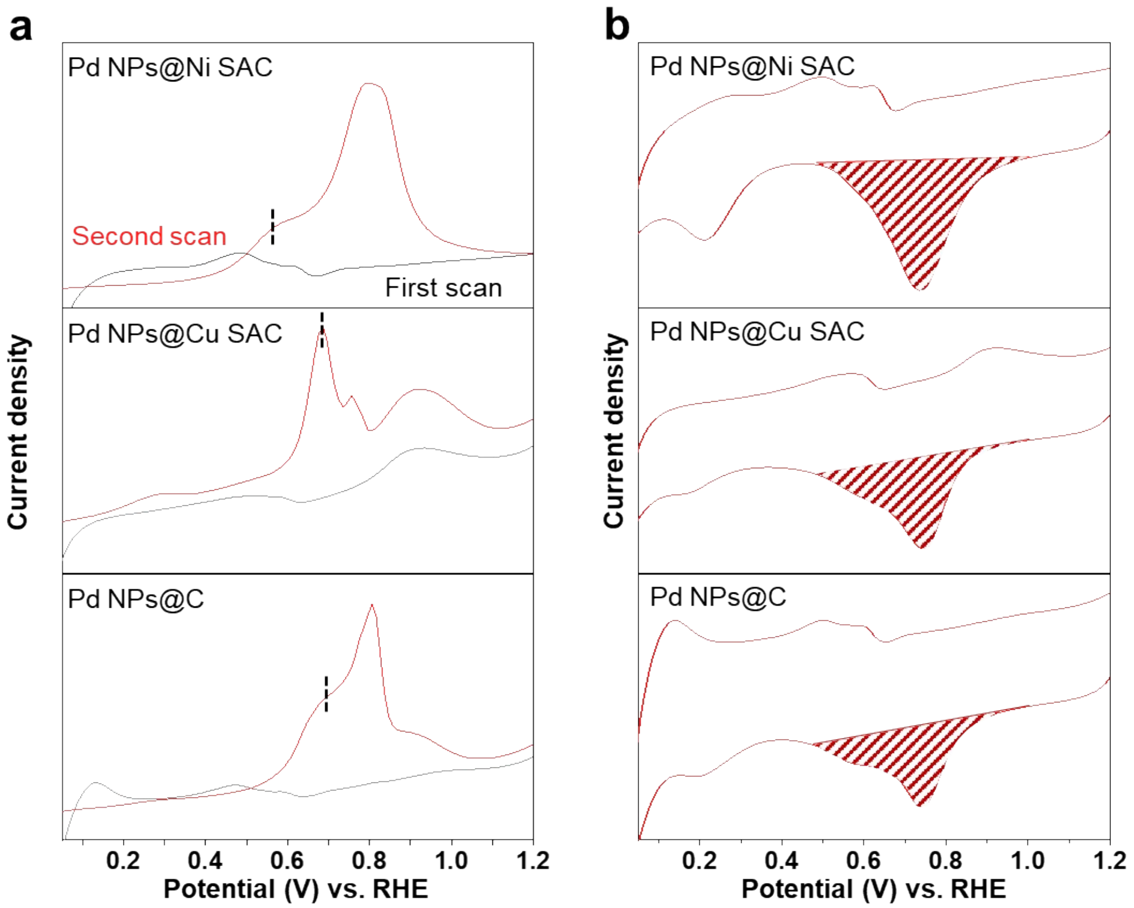

Figure S13. (a) CO stripping measurements of Pd NPs@Ni SAC, Pd NPs@Cu SAC, and Pd NPs@C at 10 mV·s^{-1} in 1 M KOH. (b) CV curve of Pd NPs@Ni SAC, Pd NPs@Cu SAC, and Pd NPs@C at 20 mV·s^{-1} in Ar-saturated 1 M KOH.

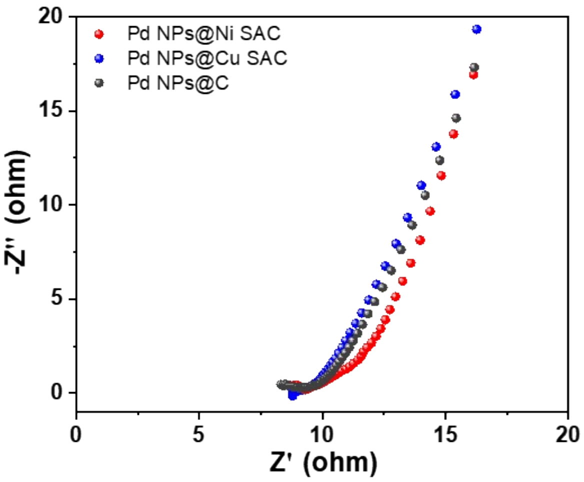

Figure S14. Electrochemical impedance spectroscopy measurement of Pd NPs@Ni SAC, Pd NPs@Cu SAC and Pd NPs@C.

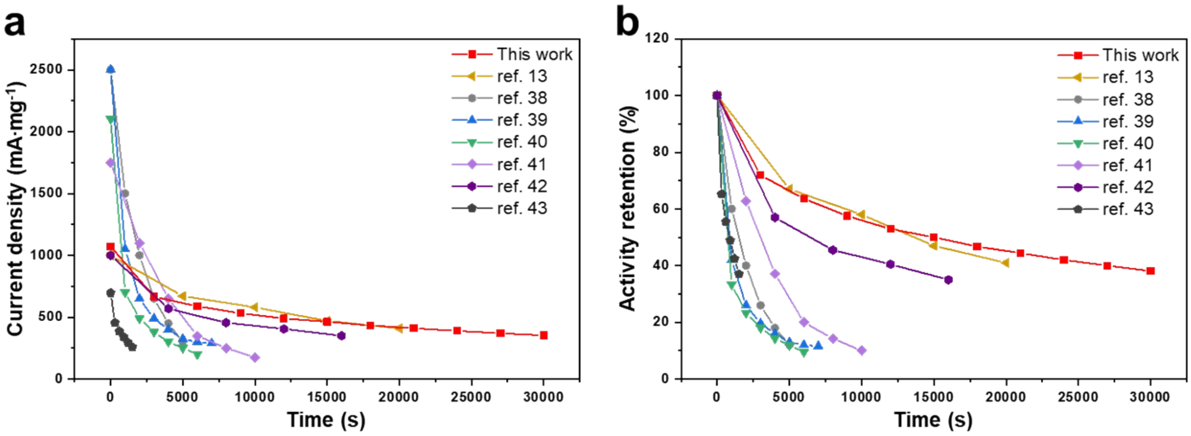

Figure S15. (a) Comparison of the EOR current density stability over time on different catalysts. The data points were obtained from the graphs of chronoamperometric tests results from different literatures and reproduced. (b) Comparison of electrochemical activity retention over time on different catalysts in EOR. The data points in Figure S15b were calculated from Figure S15a. All the literatures compared here were cited by the reference list in the main article.

Table S1. Pd, Ni and Cu contents in Pd NPs@Ni SAC, Pd NPs@Cu SAC, and Pd NPs@C tested by inductive coupled plasma (ICP) measurements.

Sample	Element	wt/100%
Pd NPs@Ni SAC	Pd	44.7
	Ni	0.9
Pd NPs@Cu SAC	Pd	43.5
	Cu	1.9
Pd NPs@C	Pd	39.1

Table S2. Pd, Ni and Cu contents in Pd NPs@Ni SAC, Pd NPs@Cu SAC, Pd NPs@C, and Ni SAC tested by XPS.

Sample	Element	*a.c./100%	wt/100%
Pd NPs@Ni SAC	Pd	3.90	25.18
	Ni	0.33	1.18
Pd NPs@Cu SAC	Pd	4.12	26.18
	Cu	0.32	1.22
Pd NPs@C	Pd	4.54	27.47
Ni SAC	Ni	0.66	3.10

*a.c./100%: atomic percent contents

Table S3. C and O contents in Pd NPs@Ni SAC, Pd NPs@Cu SAC, Pd NPs@C and Ni SAC tested by XPS.

Sample	Element	a.c./100%	wt/100%
Pd NPs@Ni SAC	C	74.77	54.64
	O	19.46	18.96
Pd NPs@Cu SAC	C	73.62	52.96
	O	20.49	19.65
Pd NPs@C	C	73.27	50.18
	O	20.65	18.89
Ni SAC	C	89.63	86.04
	O	8.46	10.83

Table S4. Structural parameters of Pd NPs@Ni SAC obtained from EXAFS fittings.

Sample	Pd NPs@Ni SAC
Structure	NiO
Scattering path	Ni-O
R (Å)	2.084±0.041
CN	6
σ^2	0.005
E_0 shift (eV)	-0.904
S_0^2	0.742
R-factor	0.013